2021 43rd Annual International Conference of the
IEEE Engineering in Medicine & Biology Society (EMBC)
Oct 31 - Nov 4, 2021. Virtual Conference

# MR Conditionality of Abandoned Leads from Active Implantable Medical Devices at 1.5T*

Yu Wang, Ran Guo, Wei Hu, Jay Jiang, Wolfgang Kainz and Ji Chen

***Abstract*—During Magnetic Resonance (MR) scans, abandoned leads from active implantable medical devices (AIMDs) can experience excessive heating near the lead-tip, depending on the types of termination applied to the proximal end. The influence of different proximal treatments, i.e., (i) freely exposed in the tissue, (ii) capped with metallic material, and (iii) capped with plastic material on the RF-induced heating are studied. Abandoned leads from a sacral neuromodulation (SNM) system were investigated in this study. The device models, i.e., the transfer functions, for different proximal treatments were developed. These models are then used to assess the in-vivo lead-tip heating inside four virtual human models (FATS, Duke, Ella, and Billie). The RF-induced heating from these abandoned leads with different proximal end treatments are compared with the lead-tip heating of the original AIMD system. The maximum lead-tip heating for abandoned leads using metal cap at the proximal end is lower than that from the original intact AIMD system. Abandoned leads with plastic cap treatment at the proximal end will lead to an average in-vivo temperature that is 3.5 times higher than that from the original intact AIMD system. Therefore, from this study and in terms of the RF-induced heating, the abandoned leads with metallic cap treatment at the proximal end can maintain the MR conditionality of the original AIMD system.**

***Clinical Relevance*— The different treatments of proximal end of the abandoned leads from AIMD are studied to ensure that MR Conditional AIMD leads remain MR Conditional when the leads are abandoned in the patients.**

## I. Introduction

Magnetic Resonance Imaging (MRI) is a widely used diagnostic tool because it can generate high-quality images for soft tissues without ionizing radiation [1]. However, for patients with active implantable medical devices (AIMDs) the radiofrequency (RF)-induced tissue heating at the distal electrodes of the AIMDs, i.e., the lead-tip, can result in thermal tissue damage [2]. To understand RF-induced lead-tip heating, numerous studies have been conducted for different AIMDs such as sacral neuromodulation (SNM) systems, and spinal cord stimulation (SCS) systems. These studies have shown that the AIMD lead acts as an "antenna", interacting strongly with the RF field generated by MR RF coils during an MR scan. Such interactions can lead to concentrated energy deposition at the lead-tip, resulting in RF-induced tissue heating around the lead-tip and possible tissue damage [3].

To ensure patient safety MR Conditional labeling is required for all AIMDs. This labeling provides the conditions under which patients can be scanned safely [4], [5]. For RF-induced heating concerns, the labeling condition should be developed based on the methods described in ISO/TS 10974, [6] in which both numerical in-vivo modeling and experimental development of AIMD models need to be performed. The developed MR Conditional labeling is always developed for the entire AIMD system, i.e., the implantable pulse generator (IPG) connected to the lead(s). However, due to IPG malfunction, battery problems, or medical reasons the IPG may need to be removed, leaving behind a functional intact and undamaged lead in the original implanted region [7]–[9]. We refer to these undamaged functional leads remaining inside the patient as abandoned leads. The MR Conditional labeling of many AIMDs instructs the user to 'cap' the abandoned lead after removing the IPG, thereby electrically insulating the proximal lead end. The proximal insulation of the abandoned lead changes the RF-induced heating at the distal end by establishing an open circuit for the RF-induced current at the proximal end. In several phantom studies at 1.5T (64 MHz), it was reported that the RF-induced lead-tip heating results from a complete AIMD cannot readily be applied to abandoned leads, and the RF-induced lead-tip heating of abandoned leads significantly depends on the type of proximal end, i.e., either capped and electrically insulated or the proximal end of the lead is in electrical contact with the surrounding tissue [10]–[13].

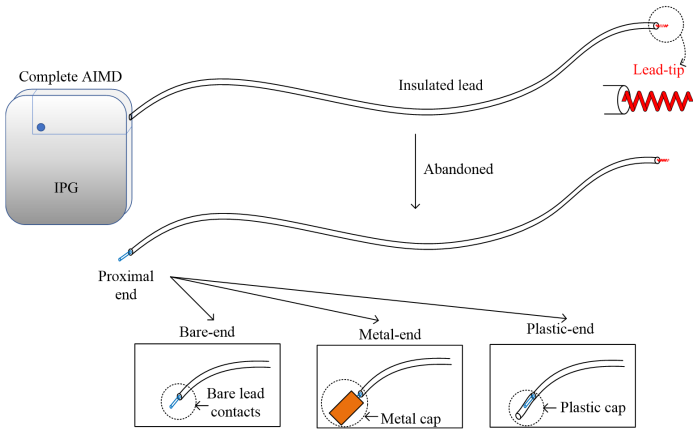


Figure **Error! Main Document Only.**. Illustration of the complete AIMD and the abandoned lead with three different types of proximal ends: Bare-end, Metal-end, and Plastic-end.

Yu Wang, Ran Guo, Wei Hu and Ji Chen are with the Department of Electrical and Computer Engineering, University of Houston, Houston, TX 77204-4005, USA (corresponding author e-mail: jchen18@uh.edu, 713-743-4423). Jay Jiang is with Axonics Inc., 26 Technology Dr., Irvine CA 92618 (e-mail: gjiang@axonics.com). Wolfgang Kainz is with Center for Devices and Radiological Health, Food and Drug Administration, Silver Spring, MD 20993, USA (e-mail: Wolfgang.Kainz@fda.hhs.gov).

This comprehensive study aims to assess the impact of the proximal end treatments of abandoned AIMD leads on the RF-induced lead-tip heating at 64 MHz (1.5T). We use an SNM system. For each abandoned AIMD lead three different proximal end treatments were considered. These three treatments are (1) Bare-end treatment, i.e., the abandoned lead's proximal end is freely exposed to the surrounding tissue once the IPG is removed, (2) Metal-end treatment., i.e., the abandoned lead's proximal end is capped with metallic material, and (3) Plastic-end treatment, i.e., the abandoned lead's proximal end is capped with an insulating material, such as plastic. The RF-induced lead-tip heating of these abandoned leads is then compared to the complete AIMD, i.e., the lead connected to the IPG. Illustrations of the three proximal end treatments are shown in Fig. 1.

## II. Method

### A. Transfer function method

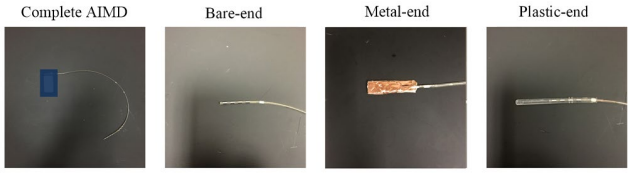


Figure 1. Illustrations of the complete AIMD and abandoned leads with different proximal end treatments. The blue rectangle is used to mask the IPG names.

The state-of-the-art method to evaluate the RF-induced in-vivo lead-tip heating is the Tier 3 TF approach described in ISO/TS 10974 Clause 8 [6], [14]. The procedure consists of two steps: (1) electromagnetic (EM) simulations to compute the electric (E)-field distributions inside anatomically correct models of the human body exposed to an MR RF coil, and (2) developing the lead model by measuring, calibrating, and validating the TF. Then the RF-induced lead-tip heating $\Delta T$ can be computed using

$$\Delta T = A\left|\int_0^L \mathrm{TF}(l)E_{tan}(l)dl\right|^2, \qquad (1)$$

where TF($l$) is the lead model, often referred to as the lead TF, $E_{tan}(l)$ is the tangential E-field along clinically relevant lead trajectories, and $A$ is a scaling coefficient.

The AIMD systems used in this study are shown in Fig. 2. They are referred to as the complete AIMD which consists of an IPG, an insulated lead with one or more metallic inner conductors, and the lead-tip electrodes contacting the tissue to be stimulated. When the IPG is removed, the abandoned lead was configurared with the three different proximal end treatments. For the Metal-end treatment, a copper sheet with dimensions of ~ 2 cm × ~ 0.5 cm was connected to the proximal lead contacts of the abandoned lead using conductive glue. For the Plastic-end treatment the proximal lead contacts of the abandoned lead were inserted into an insulated plastic tube and sealed with non-conductive glue. The copper sheet and the conductive glues are not biocompatible, these materials were chosen to ensure good electrical conductivity to demonstrate the concept. In practice, titanium or platinum and other compatibility materials would be used.

The lead TF($l$) was measured using a measurement system based on the reciprocity theorem [15], [16]. As shown in Fig. 3(A), the center conductor of a SubMiniature version A (SMA) connector was exposed and placed near the lead-tip as the excitation source. The SMA cable was connected to the output port of a vector network analyzer (VNA). A current probe was used to measure the magnitude and phase of the induced current distribution along the lead with a special resolution of 1 cm, i.e., the TF($l$). The TF($l$) measurements were performed with the full AIMD systems or the abandoned leads placed in saline with a conductivity of 0.47 S/m.

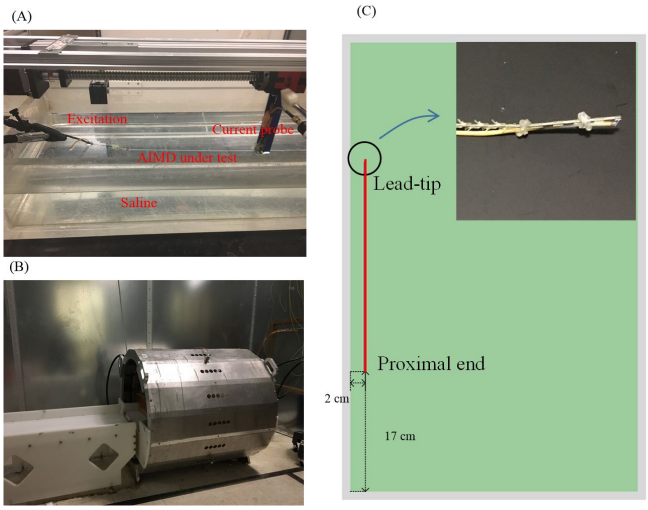


Figure 2. (A) Illustration of the TF measurement setup, (B) MITS 1.5T RF coil, (C) calibration trajectories of AIMD leads in the ASTM phantom, and photos of lead-tips and thermal probes for the SNM system.

The MITS 1.5T RF coil manufactured by Zurich Med Tech (ZMT), as shown in Fig. 3(B), was used to generate the RF exposure to obtain the scaling coefficient A in (1). The standard ASTM phantom was filled with gelled saline made of polyacrylic acid (PAA), with a conductivity of 0.47 S/m and a relative dielectric constant of 78. The exposure level was measured using calorimetry with a duration of 15 minutes. The lead trajectories in the ASTM phantom are shown in Fig. 3(C) for the AIMDs with the respective leads. The temperature probes were closely bonded to the lead-tip to measure the temperature rises near the distal lead-tip.

### B. EM simulations and AIMD lead trajectory development

The tangential E-fields along clinically relevant trajectories $E_{tan}(l)$ were calculated for four Virtual Population models. The selected models are the adult obese male model (FATS, 37 yrs, Body Mass Index (BMI) 36.1), the adult male model (Duke, 34 yrs, BMI 22.4), the adult female model (Ella, 26 yrs, BMI 21.6), and the petite young girl model (Billie, 11 yrs, BMI 15.3) [17]. These models are shown in Fig. 4(A)-(D).

The RF coil emissions were calculated for two non-physical birdcage coils operating at 64 MHz (1.5T). The larger coil was used for the obese male model FATS; it has a length of 650 mm, a diameter of 700 mm, and 16 rungs. The smaller coil was used for the other three models; it had a length of 650 mm, a diameter of 630 mm, and 16 rungs. Circularly polarized

RF fields were generated inside both RF coils. Fig. 4(E) illustrates a typical placement of Duke inside the RF coil for the EM simulations. For each human body model 63 landmarks, using 25 mm step size and spanning 1200 mm along the vertical direction were defined. The landmark position 0 mm corresponds to the center of the eyes for each human body model. The landmark 1000 mm corresponds to the position near the thigh for the adult models. To calculate the RF-induced lead-tip heating for all possible imaging conditions we computed $E_{tan}(l)$ for all models, all landmarks, and all clinically relevant lead trajectories.

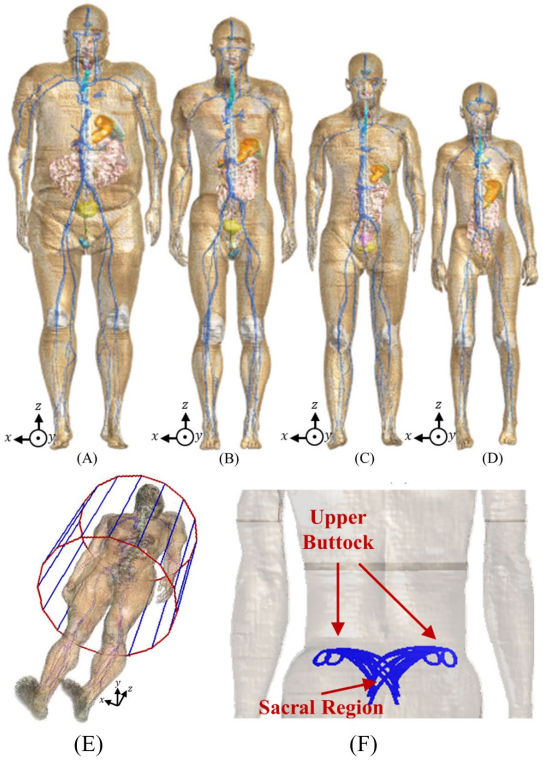


Figure 3. Illustration of the adult obese male model FATS (A), the adult male model Duke (B), the adult female model Ella (C), and the petite young girl model Billie (D). (E) shows Duke within the generic 1.5T RF coil. (F)Developed lead trajectories of the SNM system in the Duke model.

These trajectories were developed based on fluoro images from clinical applications. For the SNM system 24 trajectories were developed, i.e., 6 lead-tip locations (3 at each side of the body) and 4 IPG locations (2 at each side of the body). To account for potential patient movements each of the trajectories were shifted ± 2 mm in all three directions, resulting in 4704 trajectories for each model, or a total of 18816 evaluated lead trajectories. The trajectories for the SNM system are shown in Fig. 4(F) for the adult male model Duke.

## III. Result

### A. TF measurement result

The TFs from three AIMD systems and abandoned leads with three different proximal end treatments were developed. To obtain the scaling coefficient A in (1) the abandoned leads with the different proximal end treatments were placed along the in-vitro trajectories shown in Fig. 3(C). With the lead-tip temperature rises and the incident E-fields along the three trajectories the scaling coefficient $A$ can be determined. The magnitude and phase of these TFs are shown in Fig. 5, indicating that the shapes of the TFs of the complete AIMD and the Metal-end abandoned leads were very similar for all three AIMD systems. The magnitudes of the Metal-end abandoned lead TF models were slightly lower than those for the complete AIMDs. The magnitude of the TF for the abandoned leads with Plastic-end is close to zero at the proximal because the plastic cap eliminates the current flow into the gel.

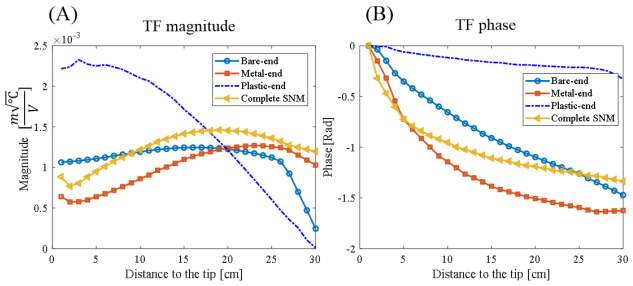


Figure 4. TFs of the complete AIMDs and abandoned AIMD leads with different proximal end treatments are shown in (A) the magnitude of the TFs for the SNM system, (B) the phase.

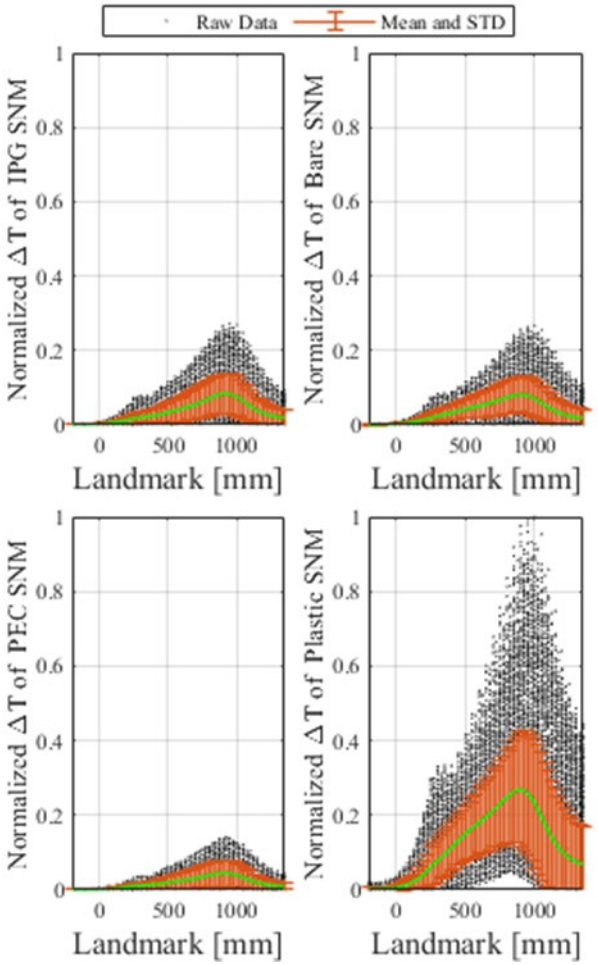


Figure 5. In-vivo lead-tip heating for the complete AIMD and the abandoned leads with three different proximal treatments at all imaging landmarks. The black dots are the calculated lead-tip heating for each lead trajectory; the red dots are the mean values with

standard deviation (STD) at each landmark. The results are normalized to the maximum in-vivo lead-tip heating.

### B. Calculating the in-vivo temperature rise

With the measured TFs of three AIMD systems and the extracted tangential E-field along different trajectories in each human model, the in-vivo temperature rises were calculated using equation (1). The RF-induced heating along different trajectories inside four human body models, as a function of landmark position, is shown in Fig. 6. The RF-induced heating at the lead-tip from the abandoned leads and the complete AIMD are shown. Each black dot represents the calculated lead-tip heating for a specific AIMD trajectory and a specific landmark. The lead-tip heating is normalized to the maximum calculated temperature rises of all cases four configurations, i.e., the complete AIMD and the abandoned leads with three different proximal end treatments. Statistical analysis was performed at each landmark to calculate the mean and standard deviation (STD) of the lead-tip heating. As clearly shown in Fig. 6, the abandoned leads of the AIMD system with Metal-end results always in lower averaged and maximum lead-tip heating compared to the complete AIMD. One can also see that abandoned leads with Plastic-end have 2 - 3 times higher mean lead-tip heating compared to the complete AIMD. Abandoned leads with Bare-end have pretty similar average lead-tip heating as the complete AIMD.

## IV. Conclusion

Numerical and experimental studies were performed to assess the RF-induced in-vivo lead-tip heating for abandoned leads with three different proximal end treatments: Bare-end, Metal-end, and Plastic-end. TF models together with in-vivo simulation results from four human body models were used to estimate the RF-induced heating from distal end for these abandoned leads. The results show that abandoned leads with Metal-ends always have lower maximum and averaged RF-induced heating compared to the complete AIMD. For abandoned leads with Bare-ends the RF-induced lead-tip heating is similar to the complete AIMD. However, abandoned leads with Plastic-ends are prone to significantly higher RF-induced lead-tip heating when compared to the complete AIMD. For patients with abandoned leads with Plastic-ends or Bare-ends the MR conditions for safe scanning need to be re-evaluated, because the RF-induced heating for some exposure scenarios can be higher than for their complete AIMD. For patients with abandoned leads with Metal-ends safe scanning using the existing MR Conditional labeling seems possible.

## Disclaimer

The mention of commercial products, their sources, or their use in connection with material reported herein is not to be construed as either an actual or suggested endorsement of such products by the Department of Health and Human Services.

## References


[1] F. G. Shellock and J. V. Crues, "MR Procedures: Biologic Effects, Safety, and Patient Care," *Radiol.*, vol. 232, no. 3, pp. 635–652, 2004.

[2] R. Guo *et al.*, "Computational and experimental investigation of RF-induced heating for multiple orthopedic implants," *Magn. Reson. Med.*, vol. 82, no. 5, pp. 1848–1858, 2019.

[3] Y. Wang *et al.*, "On the development of equivalent medium for active implantable device radiofrequency safety assessment," *Magn. Reson. Med.*, 2019.

[4] ASTM F 2182-19e2. *Standard test method for measurement of radiofrequency induced heating near passive implants during magnetic resonance imaging. ASTM Committee F04 on Medical and Surgical Materials and Devices, Subcommittee F04.15 on Material Test Methods. West Conshohocken*, PA: ASTM International; 2019.

[5] Center for Devices and Radiological Health, "Testing and Labeling Medical Devices for Safety in the MR Environment," *U.S. Food and Drug Administration*. [Online]. Available: https://www.fda.gov/regulatory-information/search-fda-guidance-documents/testing-and-labeling-medical-devices-safety-magnetic-resonance-mr-environment. [Accessed: 27-Apr-2021].

[6] *Assessment of the safety of magnetic resonance imaging for patients with an active implantable medical device*. Standard ISO/TS 10974: 2018, Mar. 2018.

[7] P. Blomstedt and M. I. Hariz, "Hardware-related complications of deep brain stimulation: a ten year experience," *Acta Neurochirurgica*, vol. 147, no. 10, pp. 1061–1064, 2005.

[8] M. I. Hariz, P. Shamsgovara, F. Johansson, G.-M. Hariz, and H. Fodstad, "Tolerance and Tremor Rebound following Long-Term Chronic Thalamic Stimulation for Parkinsonian and Essential Tremor," *Stereotact. Funct. Neurosurg.*, vol. 72, no. 2-4, pp. 208–218, 1999.

[9] C. Joint, D. Nandi, S. Parkin, R. Gregory, and T. Aziz, "Hardware-Related problems of deep brain stimulation," *Mov. Disord.*, vol. 17, no. S3, 2002.

[10] D. A. Langman, I. B. Goldberg, J. P. Finn, and D. B. Ennis, "Pacemaker lead tip heating in abandoned and pacemaker-attached leads at 1.5 tesla MRI," *J. Magn. Reson. Imaging*, vol. 33, no. 2, pp. 426–431, 2011.

[11] E. Mattei, G. Gentili, F. Censi, M. Triventi, and G. Calcagnini, "Impact of capped and uncapped abandoned leads on the heating of an MR-conditional pacemaker implant," *Magn. Reson. Med.*, vol. 73, no. 1, pp. 390–400, 2014.

[12] C. Balmer, M. Gass, H. Dave, F. Duru, and R. Luechinger, "Magnetic resonance imaging of patients with epicardial leads: in vitro evaluation of temperature changes at the lead tip," *J. Interv. Card. Electrophysiol*, vol. 56, no. 3, pp. 321–326, 2019.

[13] R. Guo, J. Zheng, Z. Wang, R. Yang, J. Chen, and T. Hoegh, "Reducing the Radiofrequency-Induced Heating of Active Implantable Medical Device with Load Impedance Modification," *presented at the 2020 Int. Antennas Propag. Soc. Int. Symp.*, Montreal, QC, Canada, July 5–10, 2020.

[14] S. M. Park, R. Kamondetdacha, and J. A. Nyenhuis, "Calculation of MRI-induced heating of an implanted medical lead wire with an electric field transfer function," *J. Magn. Reson. Imaging*, vol. 26, no. 5, pp. 1278–1285, 2007.

[15] S. Feng, R. Qiang, W. Kainz, and J. Chen, "A technique to evaluate MRI-induced electric fields at the ends of practical implanted lead," *IEEE Trans. Microw. Theory Tech.*, vol. 63, no. 1, pp. 305–313, 2015.

[16] J. Liu, J. Zheng, Q. Wang, W. Kainz, and J. Chen, "A Transmission Line Model for the Evaluation of MRI RF-Induced Fields on Active Implantable Medical Devices," *IEEE Trans. Microw. Theory Tech.*, vol. 66, no. 9, pp. 4271–4281, 2018.

[17] M.C. Gosselin *et al.*, "Development of a new generation of high-resolution anatomical models for medical device evaluation: the Virtual Population 3.0," *Phys. Med. Biol.*, vol. 59, no. 18, pp. 5287–5303, 2014.